

The inverse dielectric function of a quasi-two-dimensional electron gas in a quantum well:
plasmons in a thin metal layer

This article has been downloaded from IOPscience. Please scroll down to see the full text article.

1996 J. Phys.: Condens. Matter 8 665

(<http://iopscience.iop.org/0953-8984/8/6/007>)

View [the table of contents for this issue](#), or go to the [journal homepage](#) for more

Download details:

IP Address: 171.66.16.179

The article was downloaded on 13/05/2010 at 13:10

Please note that [terms and conditions apply](#).

The inverse dielectric function of a quasi-two-dimensional electron gas in a quantum well: plasmons in a thin metal layer

K León-Monzón[†], H Rodríguez-Coppola[†], V R Velasco[‡] and
F García-Moliner[‡]

[†] Departamento de Física Teórica, Facultad de Física, Universidad de la Habana, San Lázaro y L, Vedado, Havana, Cuba

[‡] Instituto de Ciencia de Materiales, CSIC, Serrano 123, 28006 Madrid, Spain

Received 25 October 1995

Abstract. A formal expression for the energy-loss function of a fast electron interacting with an inhomogeneous quasi-2D electron gas in a quantum well is given in the quasiclassical approximation. It uses the non-local inverse dielectric function derived in a previous paper. As an illustrative example, the plasmon dispersion relations of a thin metal film embedded in dielectric caps are calculated, taking into consideration the influence of the empty part of the electronic spectrum, the dielectric discontinuity of the system and the influence of various occupied subbands. By following the peaks of the loss function, rather than seeking zeros of the secular determinant, one can easily obtain the plasmon branches even when these enter the domains of Landau damping. For several occupied subbands the number of acoustic plasmon branches is the same as the number of occupied subbands, and the intersubband plasmon branches at $q = 0$ appear at energies close to each one of the transitions allowed in the system, which we call the leading transition of the plasmon branch. The depolarization effect is shown to be strongly dependent on the population of the system and on the type of the leading transition involved, i.e. a leading transition between occupied subbands or between one occupied and one empty subband. Some regularities for this effect are observed, correlating the depolarization energy with the order of the states involved as the leading transition of the plasmon mode.

1. Introduction

The dielectric function of a quasi-2D electron gas (Q2DEG) has been extensively studied in the last twenty years [1–21] because of its paramount importance in the interpretation of some optical experiments and dielectric properties of systems like inversion layers in metal–insulator–semiconductor systems and modulation-doped heterojunctions, quantum wells and superlattices. Most of the literature on the subject is devoted to studying the RPA dielectric function for such systems. In the lowest approximation the electron gas is taken to be strictly 2D, which leaves only one band of electronic states in the spectrum. Even if the spatial extent of the wavefunctions $\varphi_n(z)$ in the z -direction, perpendicular to the interfaces, is taken into account, the approximation known as the electrical quantum limit has often been made in which all the carriers are assumed to be in the lowest subband and the rest of the spectrum is ignored. In some cases the effect of some ‘virtual states’, that is, of some empty subbands above the occupied ones, is taken into account. In any case the usual approach is to work in terms of matrix elements between one-electron wavefunctions $\varphi_n(z)$

of bare and screened potentials. The dielectric function ϵ is then written in terms of this basis and, for the problem of inverting ϵ , the spectrum of one-electron states is truncated and then the inversion effected in the truncated basis.

It was stressed in [22] that since the spectrum is infinite, a formal mathematical analysis is in principle required in which one must prove the existence of a unique and bounded inverse. Such an analysis was given in general terms in [23], where a convergent algorithm was given which generates a sequence of approximations proven to converge to the exact solution. This was used to invert ϵ , in the random-phase approximation, in [22], where the approach differed from the usual one in two respects, namely: (i) the problem was solved in real space as regards the position z , that is, having been Fourier transformed in the plane $\rho = (x, y)$, which introduces a 2D wavevector \mathbf{q} , the dielectric function, written as $\epsilon(\mathbf{q}, \omega; z, z')$ was inverted as $\epsilon^{-1}(\mathbf{q}, \omega; z, z')$, so that the screened potential is obtained in real z -space as the function $V_s(\mathbf{q}, \omega; z)$ (the dependence on (\mathbf{q}, ω) will be henceforth everywhere understood when not indicated explicitly); and (ii) the basis functions were not the $\varphi_n(z)$; instead, a dual basis of *long-* and *short-range* functions was introduced, as will be indicated below. These are intrinsically more appropriate to the physics of the dielectric response and also provide a practical basis for numerical calculations. The effects of the empty subbands on the screening of an external potential were studied in [22] by direct evaluation of $V_s(z)$ in real space.

The inverse dielectric function is also crucial in the theory of the energy loss of an external fast particle [24]. Lacking an explicit formula for $\epsilon^{-1}(z, z')$, in order to study a confined inhomogeneous electron gas one must resort to approximations. In [25] the electron gas was assumed to be strictly 2D and the problem was studied in terms of the *surface response function*, a concept related to the 2D Fourier transform of ϵ^{-1} . The energy loss for a multilayer semi-infinite material was studied in [26] by starting with different frequency-dependent dielectric functions $\epsilon_j(\omega)$ —i.e. neglecting spatial dispersion—and then replacing the multilayer structure by an effective medium with an average $\epsilon(\omega)$. Spatial dispersion for an actual quasi-2D system—a finite semiconductor layer—was taken into account in [27] by making the so-called diagonal approximation, in which one neglects quantum interference effects in the description of the confined electron gas. The problem was then studied by means of Fourier transforms of the z -dependent quantities of interest.

Now, these approximations and complications can be avoided if an explicit formula for $\epsilon^{-1}(z, z')$ is available, as will be presently seen. On the other hand, the confined electron gas is usually embedded between materials of different background crystal dielectric constants. Such is the case, for instance, for the thin metal film studied in [21], which is embedded in dielectric caps. The background dielectric discontinuities are in this case substantial, and one may enquire whether taking a proper account of the background dielectric discontinuity may have appreciable consequences.

The purpose of this paper is to give a very simple derivation of an explicit formula for the energy-loss function in terms of $\epsilon^{-1}(z, z')$ and to use this to extract from its peaks the dispersion relations of the plasmons of the thin metal film studied in [21] with a view to studying the effects of (i) background dielectric discontinuities and (ii) empty subbands.

2. The inverse dielectric function

We summarize here the formula derived in [22] for $\epsilon^{-1}(z, z')$. Given any pair of functions φ_n and $\varphi_{n'}$, the *short-range function* $S_{nn'}$ is defined as

$$S_{nn'}(z) = \varphi_n(z)\varphi_{n'}(z) \quad (1)$$

and the long-range function $L_{nn'}$ by

$$L_{nn'}(z) = \int dz' G(z, z') S_{nn'}(z') \quad (2)$$

where $G(z, z')$ is the Green function for the Poisson equation in the background dielectric structure in the absence of the electron gas. The appropriateness of the $L_{nn'}(z)$ and $S_{nn'}(z')$ for forming a dual basis for non-local functions of (z, z') is clear from the physical meaning of (1) and (2): $S_{nn'}$ is an element of the density matrix and $L_{nn'}$ is the electrostatic potential created at z by a charge density $S_{nn'}(z')$. Now, in the random-phase approximation, $\epsilon(z, z')$ is of the form

$$\epsilon(z, z') = \delta(z - z') - \frac{1}{S_{xy}} \sum_{n, n'} \sum_{\kappa, \kappa'} L_{nn'}(z) P_{nn'}(\mathbf{q}, \omega) S_{nn'}(z') \quad (3)$$

where the $P_{nn'}$ are 2D, RPA polarizability terms. It proves convenient to introduce a new labelling of the terms so that each pair of discrete labels, (n, n') , becomes one discrete label μ . A convenient and physically meaningful way of carrying out this process was explained in [22]. Then, in the new labelling, the inverse dielectric function $\epsilon^{-1}(z, z')$ satisfying the condition

$$\int dz'' \epsilon(z, z'') \epsilon^{-1}(z'', z') = \delta(z - z') \quad (4)$$

is

$$\epsilon^{-1}(z, z') = \delta(z - z') + \sum_{\mu\nu} L_{\mu}(z) M_{\mu\nu} S_{\nu}(z') \quad (5)$$

where the matrix \mathbf{M} of elements $M_{\mu\nu}$ is obtained as follows. Define the matrix β of elements:

$$\beta_{\mu\nu} = \int dz S_{\mu}(z) L_{\nu}(z) \quad (6)$$

and the diagonal matrix \mathbf{P} of elements $P_{\mu}\delta_{\mu\nu}$. Then the matrix \mathbf{M} is

$$\mathbf{M} = (\mathbf{I} - \mathbf{P}\beta)^{-1} \mathbf{P}. \quad (7)$$

The point to note is that the matrix to be inverted is infinite, corresponding to the fact that the spectrum of electronic states is infinite, and this in principle requires a formal mathematical analysis which must start by first proving the existence of a bounded and unique inverse. The general conditions for the existence of the inverse were established in [23], where a convergent algorithm was obtained. This justifies the process in which one *first* truncates the infinite matrix—i.e. the electronic spectrum—and *then* inverts while establishing an algorithm which generates a sequence of results for the successive truncations which converges to the exact answer. This was applied in [22] to the inversion of ϵ in the manner summarized above.

Now, the long-range functions $L_{\mu}(z)$ contain the Green function of the Poisson equation, as seen in equation (2). If the background crystal is homogeneous, then $G(z, z')$ is simply

$$G(z, z') = \frac{2\pi e^2}{q\epsilon_x} e^{-q|z-z'|} \quad (8)$$

but if one wants to study a general sandwich type of structure A–B–C, where A and C may or may not be equal, but they are in any case different from B, where the confined electron gas is contained, then one wants G for the background dielectric heterostructure ϵ_1 – ϵ_2 – ϵ_3 , where ϵ_1 and ϵ_3 may or may not be equal but are different from ϵ_2 . The corresponding

G can be readily obtained in exact form by using the method of surface Green function matching [28]. The result is

$$G(z, z') = \frac{2\pi e^2}{q} e^{-q|z-z'|} g(z, z') \quad (9)$$

with $g(z, z')$ given by:

$$g(z, z') = \begin{cases} g_3 H_1(z') + h_2(1 - H_1(z')) G_1(z') & z \in A, z' \in B \\ g_1 G_1(z') + h_2(K_1(z') - 1) H_1(z') & z \in C, z' \in B \\ g_3 H_1(z) + h_2(1 - H_1(z)) G_1(z) & z \in B, z' \in A \\ g_1 G(z) + h_2(K_1(z) - 1) H_1(z) & z \in B, z' \in C \\ (1/G_1(d)) [(1/\epsilon_2) G_1(z) H_1(z') \\ + (1/\gamma)(K_1(d) - 1) S_1(q; z, z')] & z, z' \in B; z \leq z' \\ (1/G_1(d)) [(1/\epsilon_2) H_1(z) G_1(z') \\ + (1/\gamma)(K_1(d) - 1) S_2(q; z, z')] & z, z' \in B; z' \leq z \\ (1/\epsilon_1) [1 + e^{q|z-z'|} e^{q(z+z')} [h_1 \gamma_{32} G_1(d) - 1]] & z, z' \in A \\ (1/\epsilon_3) [1 + e^{2qd} e^{q|z-z'|} e^{q(z+z')} [h_3 \gamma_{12} G_1(d) - 1]] & z, z' \in C \\ h_2 G_1(d) & z \in A, z' \in C \\ & \text{or vice versa} \end{cases}$$

where

$$\begin{aligned} H_1(z) &= 1 - e^{-2q(d-z)} & G_1(z) &= 1 - e^{-2qz} & K_1(z) &= 1 + e^{-2qz} \\ g_1 &= 2 \frac{\gamma_{12}}{\gamma} & g_3 &= 2 \frac{\gamma_{32}}{\gamma} \\ h_1 &= 4 \frac{\epsilon_1}{\gamma} & h_2 &= 4 \frac{\epsilon_2}{\gamma} & h_3 &= 4 \frac{\epsilon_3}{\gamma} \\ \gamma &= G_1(d) [(\epsilon_1 \epsilon_3 + \epsilon_2^2) G_1(d) + \epsilon_2(\epsilon_1 + \epsilon_3) K_1(d)] \\ \gamma_{12} &= \epsilon_1 G_1(d) + \epsilon_2 K_1(d) & \gamma_{32} &= \epsilon_3 G_1(d) + \epsilon_2 K_1(d) \\ S_1(q; z, z') &= e^{-2q(z-z')} H_1(z) G_1(z') + G_1(z) H_1(z') + Q(z, z') \\ S_2(q; z, z') &= e^{2q(z-z')} G_1(z) H_1(z') + H_1(z) G_1(z') + Q(z, z') \\ Q(z, z') &= 0.5 \left[\gamma_{32} e^{2q(d-z)} H_1(z) H_1(z') + \gamma_{12} e^{2qz'} G_1(z) G_1(z') \right]. \end{aligned}$$

3. The power loss

Once an explicit formula for $\epsilon^{-1}(z, z')$ is available it is a simple matter to obtain another explicit formula for the power loss of a fast external moving charge in interaction with the confined electron gas. It was shown in [29] that the full quantum-mechanical analysis does not really add anything new to the semi-classical treatment [24] in which the external fast particle is described classically. This approach will be used here.

We consider a reflecting trajectory in which an external fast electron constitutes an external charge density:

$$\sigma_0(\mathbf{r}, t) = -e\delta(\mathbf{r} - \mathbf{V}t) \tag{10}$$

where the velocity

$$\mathbf{V} = \mathbf{w} + \mathbf{u} \tag{11}$$

has a constant parallel component w and a perpendicular component

$$\mathbf{u}(t) = [u\theta(-t) - u\theta(t)] \mathbf{z}^0 \tag{12}$$

which changes sign at $t = 0$, when the Heaviside step function θ changes sign. We consider three cases, namely (a) where $w \neq 0$ and $u \neq 0$, (b) where $u = 0$, $\mathbf{V} = \mathbf{w}$ and (c) where $w = 0$, $\mathbf{V} = \mathbf{u}$. The 2D Fourier transform of the external charge density is

$$\sigma_0(\mathbf{q}, \omega, \mathbf{V}, z) = -e \begin{cases} (2/u) \cos[(\alpha/u)z] & \text{case (a)} \\ 2\pi\delta(\alpha)\delta(z - z_0) & \text{case (b)} \\ (1/u)e^{i\omega z/u} & \text{case (c)} \end{cases} \tag{13}$$

where

$$\alpha = \omega - \mathbf{q} \cdot \mathbf{w} \tag{14}$$

and z_0 is the constant value of z for the parallel trajectory ($u = 0$). This produces an external potential:

$$\Phi_0(\mathbf{q}, \omega, \mathbf{V}, z) = \int dz' G_P(\mathbf{q}, z, z')\sigma(\mathbf{q}, \omega, \mathbf{V}; z') = -e\psi(\mathbf{q}, \omega, \mathbf{V}, z). \tag{15}$$

This defines ψ . The induced potential, accounting for the response of the confined electron gas, is

$$\Phi_I(\mathbf{q}, \omega, \mathbf{V}, z) = -e \sum_{\mu\nu} L_\mu(\mathbf{q}, z) M_{\mu\nu}(\mathbf{q}, \omega) U_\nu(\mathbf{q}, \omega, \mathbf{V}) \tag{16}$$

where

$$U_\nu(\mathbf{q}, \omega, \mathbf{V}) = \int dz' S_\nu(z')\psi(\mathbf{q}, \omega, \mathbf{V}, z'). \tag{17}$$

On Fourier transforming back in 2D from \mathbf{q} to $\boldsymbol{\rho} = (x, y)$, we have $\Phi_I(\boldsymbol{\rho}, \omega, \mathbf{V}; z)$, whence the total energy loss is given by

$$W = -e \int_{-\infty}^{\infty} dt \mathbf{V} \cdot \nabla \Phi_I(\boldsymbol{\rho}, \mathbf{V}, z, t)|_{r=\mathbf{V}t}. \tag{18}$$

On Fourier transforming in 1D from $L_\mu(\mathbf{q}, z)$ to $L_\mu(\mathbf{q}, k)$ this yields (taking into consideration that $\mathbf{Q} = \mathbf{q} + k\mathbf{z}^0$):

$$W = \frac{e^2}{(2\pi)^3} \text{Im} \left\{ \int d^2\mathbf{q} \int d\omega \int dk [\mathbf{Q} \cdot \mathbf{V}] \delta[\mathbf{Q} \cdot \mathbf{V} - \omega] \right. \\ \left. \times \sum_{\mu\nu} L_\mu(\mathbf{q}, k) M_{\mu\nu}(\mathbf{q}, \omega) U_\nu(\mathbf{q}, \omega, \mathbf{V}) \right\} \tag{19}$$

whence equating this to

$$W = \int d^2\mathbf{q} \int \omega d\omega P(\mathbf{q} \cdot \boldsymbol{\omega}) \tag{20}$$

we obtain the power loss function:

$$P(\mathbf{q}, \omega) = -\frac{e^2}{(2\pi)^3} \left\{ \begin{array}{l} \frac{\pi}{u^2} \operatorname{Im} \left[\sum_{\mu\nu} \left(L_\mu \left(\mathbf{q}, \frac{\mathbf{q} \cdot \mathbf{w} - \omega}{u} \right) \right. \right. \\ \left. \left. - L_\mu \left(\mathbf{q}, \frac{\omega - \mathbf{q} \cdot \mathbf{w}}{u} \right) \right) \right] \\ \times M_{\mu\nu}(\mathbf{q}, \omega) U_\nu(\mathbf{q}, \omega, \mathbf{V}) \end{array} \right] \quad \text{case (a)} \\ \\ 2\pi \operatorname{Im} \left[\sum_{\mu\nu} L_\mu(\mathbf{q}, z_0) M_{\mu\nu}(\mathbf{q}, \omega) U_\nu^0(\mathbf{q}, z_0) \right] \quad \text{case (b)} \\ \\ \frac{1}{u^2} \operatorname{Im} \left[\sum_{\mu\nu} L_\mu(\mathbf{q}, \omega/u) M_{\mu\nu}(\mathbf{q}, \omega) U_\nu(\mathbf{q}, \omega, u) \right] \quad \text{case (c).} \end{array} \right. \quad (21)$$

The quantity U^0 of case (b) is defined by

$$U_\nu(\mathbf{q}, \omega, \mathbf{w}) = 2\pi \delta(\omega - \mathbf{q} \cdot \mathbf{w}) U_\nu^0(\mathbf{q}, z_0). \quad (22)$$

This provides a formula for the calculation of the power loss which uses directly the explicit formula for $\epsilon^{-1}(z, z')$.

As a useful byproduct one can obtain from here the normal modes of the confined electron gas.

4. Plasmons in a thin metal film

We now consider plasmons in a thin metal film, the problem studied in [21], where up to two occupied subbands and some empty ones were included in the calculations. The film thickness is $d = 23.9 \text{ \AA}$ and the quantum well is assumed to have infinite barriers. The 2D polarizability elements can then be easily obtained analytically as functions of (\mathbf{q}, ω) [21]. The plasmon dispersion relations can be obtained either from the zeros of the secular determinant [22]:

$$\det|M_{\mu\nu}(\mathbf{q}, \omega)| = 0 \quad (23)$$

or from the peaks of the loss function. In the first case the analysis of [22] provides a direct physical interpretation of the results obtained in successive approximations but this has a limitation, when a plasmon branch enters a Landau damping region in the (ω, \mathbf{q}) diagram. The zeros of (23) are then complex and tracking them soon becomes a very cumbersome numerical task, while the peaks of the loss function can sometimes be followed well into the damping region.

We followed the second procedure, with occasional checks based on a complementary study of the secular determinant (23).

Figure 1 shows the first four branches obtained for the case of one occupied subband. The total number of subbands included in the calculation was nine, which proved sufficiently accurate. In order to account for the dielectric cap we took $\epsilon_A = \epsilon_B = 1$, $\epsilon_C = 12$ and used the electrostatic Green function given in (9) with a view to studying the possible effects of the background dielectric discontinuity. The results—dashed lines—actually turn out to be very close to those obtained for $\epsilon_A = \epsilon_B = \epsilon_C$ —full lines. The maximum deviation

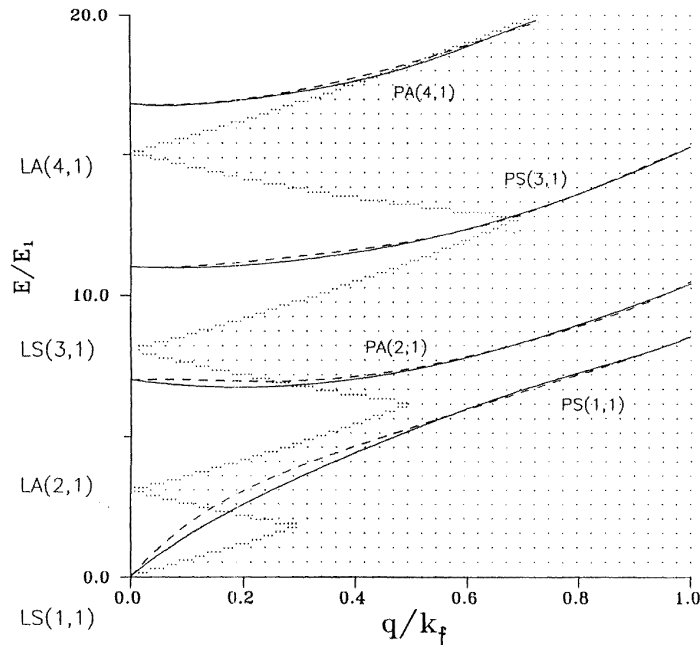


Figure 1. Plasmon dispersion relations for the first four modes of a thin metal film ($d = 23.9 \text{ \AA}$) in the infinite-barrier model. E_1 is the energy of the ground state and only the lowest subband is occupied, the Fermi energy being $E_F = 3.5E_1$. Nine subbands were included in the calculation. Full lines: $\epsilon_A = \epsilon_B = \epsilon_C = 1$. Dashed lines: $\epsilon_A = \epsilon_B = 1, \epsilon_C = 12$. The shaded regions are domains of Landau damping associated with intra- or intersubband excitations and are labelled $L(n, n')$, while the $P(n, n')$ denote the plasmon branches.

occurs for the intraband mode (1, 1) around $q = 0.2k_F$ and amounts to 8 meV, while typical experimental resolutions in EELS spectra are about 20 meV [30]. Thus the results appear to be in practice quite insensitive to the background dielectric discontinuity even though this would seem to be quite substantial; consequently from this point on we simply took $\epsilon_A = \epsilon_B = \epsilon_C = 1$ everywhere. We also note that the dispersion branches are very similar to those obtained in [21], except for the first interband mode (2, 1), which behaves quite differently for low values of q . The present result was corroborated (a) from the peak of the loss function and (b) from the zero of the secular determinant and both were in perfect agreement as long as the second method worked.

Figure 2 shows results obtained for the same situation as in figure 1—one occupied subband—but demonstrates the effects of truncating the spectrum of the electronic states. Even if only one subband is occupied it is known, both for the plasmon dispersion relation [21] and for the dynamical screening of an external potential [22], that the electrical quantum limit can be a poor approximation. Figure 2 compares the first four plasmon dispersion relations obtained when the total number of subbands included in the calculation is *nine* (full lines) or *two* (dashed lines). It suffices to show the results for the first two branches. The differences are quite substantial. For instance, for the first interband mode (2, 1) at $q = 0.2k_F$ the difference amounts to 58 meV which is sufficient to be experimentally detectable [30]. Note, incidentally, that the labels S (symmetric) and A (antisymmetric) have now been added to the band indices (n, n') , since with $\epsilon_A = \epsilon_B = \epsilon_C$ the structure is now fully symmetric.

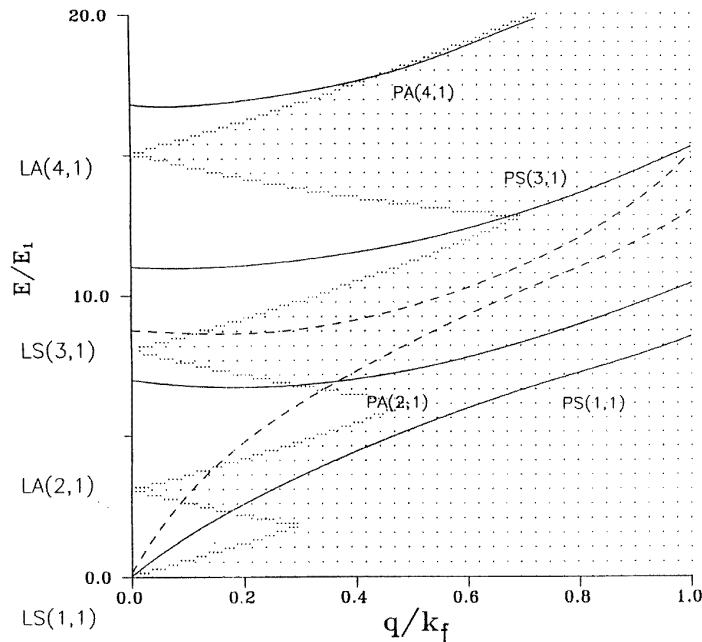


Figure 2. The same situation as in figure 1, but with $\epsilon_A = \epsilon_B = \epsilon_C$. Full lines: nine subbands included in the calculation. Dashed lines: only *two* subbands included. A new label S (for symmetric modes: $n + n'$ even) or A (for antisymmetric modes: $n + n'$ odd) has been added to $L(n, n')$ and $P(n, n')$.

As shown in [23], the formulation in terms of the $\{L_\mu(z), S_\nu(z')\}$ basis functions yields a direct factorization of the symmetric and antisymmetric parts in real space which is very useful in separating out all the results. This proves rather practical in a situation like that shown in figures 3 and 4, which show several plasmon branches, from (3, 3) in figure 3 to (6, 3) in figure 4, when three subbands are occupied and *twenty seven* are taken into account in the calculation. There are three intrasubband modes starting from $\omega = 0$, the lowest one being (3, 3) as it corresponds to the lowest population. The nature of the coupling between these modes, which is not dynamical, was discussed in [22]. We note that these three modes have the same symmetry, as $n + n'$ is even in all of them, and each one of them can decay when it is inside any intrasubband Landau damping region of ground-state subband energy larger than or equal to that of the intrasubband plasmon under discussion. Consequently the figure shows only the $LS(1, 1)$ Landau damping domain, which has the highest boundary and includes the domains $LS(2, 2)$ and $LS(3, 3)$. Thus the (3, 3) and (2, 2) intrasubband plasmon branches are fully within damping regions; although there is no numerical problem in following them up through the peaks of the loss function, which indicates that the damping is not very strong. The highest intrasubband mode (1, 1) is the only one which has a starting range in which it is fully long lived. The figures display the situation for the rest of the modes.

The intersubband plasmons (n, n') start at energies above the threshold $\Delta E_{nn'} = E_{n'} - E_n$ of the corresponding single-particle intersubband excitations due to the depolarization effect [7] arising out of the mutual screening among the electron gases in the different subbands. In the usual secular determinant approach these effects reside in the non-diagonal elements,

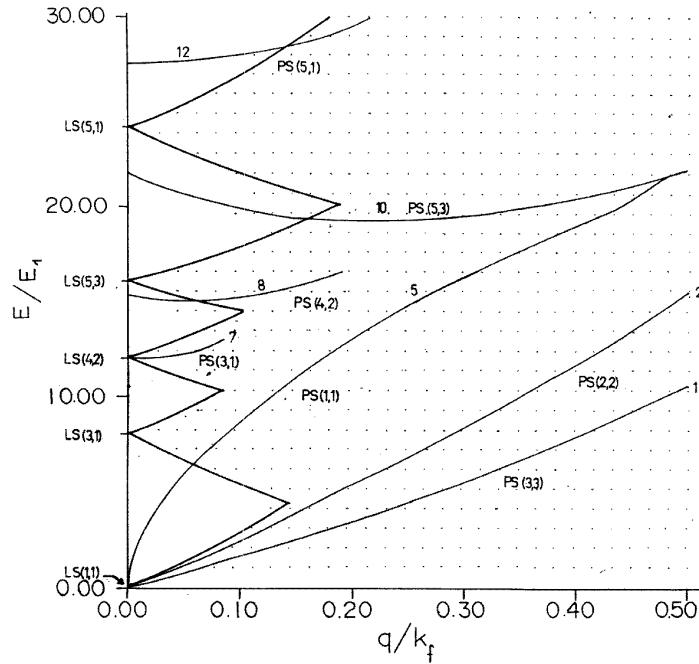


Figure 3. Symmetric plasmon branches and Landau damping domains when three subbands are occupied ($E_F = 10.5E_1$) and *twenty seven* subbands are included in the calculation.

Table 1. The depolarization energy shift (Δ_P) in units of E_1 for the different plasmon modes obtained for various numbers of occupied subbands. The transitions between occupied subbands are listed above the horizontal lines. $\Delta E_{nn'}$ is also in units of E_1 .

One occupied subbands				Two occupied subbands				Three occupied subbands				Four occupied subbands			
n	n'	$\Delta E_{nn'}$	Δ_P	n	n'	$\Delta E_{nn'}$	Δ_P	n	n'	$\Delta E_{nn'}$	Δ_P	n	n'	$\Delta E_{nn'}$	Δ_P
1	2	3	3.9	1	2	3	1.9	1	2	3	2	1	2	3	2
1	3	8	3	2	3	5	5.9	2	3	5	2	2	3	5	2
1	4	15	1.7	1	3	8	4	1	3	8	4	3	4	7	2
				2	4	12	4.9	3	4	7	4	1	3	8	3
				1	4	15	2.6	2	4	12	3.2	2	4	12	3.1
				2	5	21	2	1	4	15	3.4	1	4	15	3.9
				1	5	24	2	3	5	16	5.7	4	5	9	3
								2	5	21	5.1	3	5	16	3.4
								1	5	24	3.2	4	6	20	1.5
								3	6	27	2	2	5	21	3.9
												1	5	24	3
												3	6	27	1

which are static in nature but q -dependent and non-vanishing in the limit $q \rightarrow 0$. Table 1 displays the intersubband excitation energies $\Delta E_{nn'}$ and corresponding depolarization shifts Δ_P . Some approximate trends can be identified. For n and n' corresponding to occupied subbands, Δ_P increases as Δn increases, while in the cases when n is occupied and n' unoccupied, for fixed n' Δ_P tends to increase as Δn decreases. This holds for as long as the corresponding excitation energies are energetically ordered, which in this case occurs

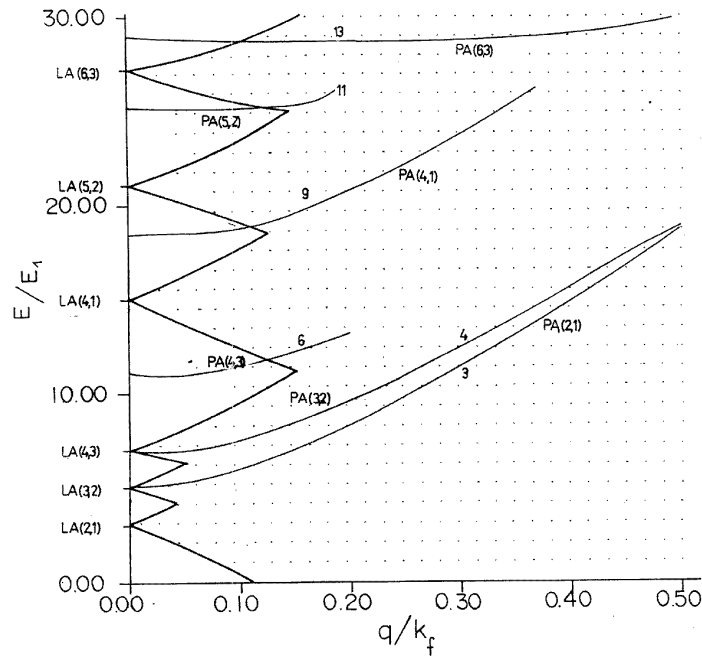


Figure 4. Antisymmetric modes for the same case as in figure 3.

for up to three occupied subbands. From then on this ordering is broken and it is difficult to identify any systematic trend.

5. Final comments

Some attempts have been made by various authors at inverting the dielectric function in real space for semi-infinite [31, 32] or superlattice [33–35] systems based on various approximations from the start. The approach of [22] is quite different. The formulation holds for a bounded inhomogeneous electron gas confined to a finite domain which could be bounded in one, two or three dimensions and is valid under quite general approximations, the only restriction being the random-phase approximation. This paper complements [22] in the study of different questions of physical interest related to the explicit inversion of $\epsilon(z, z')$ in real space for a planar structure of the quantum well type in the RPA. We find that the long- and short-range functions, besides having an appealing physical meaning, prove very practical for numerical calculations, and with the relabelling $(n, n') \rightarrow \mu$ one can easily study the effects of including any desired number of empty subbands, which actually turn out to be quite significant, as demonstrated in figure 2.

The model application worked out here serves only a demonstrative purpose but it illustrates (i) some trends in the behaviour of the depolarization shift for intersubband plasmons and (ii) the fact that, contrary to what might have seemed a plausible expectation, the effects of accounting for the background dielectric discontinuity are quite negligible, even in the case of a metal film on a dielectric cap, where one might have anticipated substantial effects.

The formulation is not restricted to the infinite-barrier model and one could equally start

from more accurate electronic wavefunctions for a more realistic calculation, as long as the RPA is acceptable for the problem under study. The interesting question now is that of how to improve upon the RPA. This is not a trivial matter for the bounded inhomogeneous electron gas, but one may expect that since there is no reason for the long- and short-range one-electron wavefunctions to be in any way different, one may find the same mathematical structure as reflected in (3) with different 2D polarizabilities. The formal mathematical basis and the practical algorithms developed in [23] and used in [22] and here could then be equally employed and one may anticipate that once the new 2D polarizabilities have been obtained, the closed expression for the improved $\epsilon(z, z')$ will have a similar form. Work on this problem is currently going on in our group.

Acknowledgment

This work was partially supported by the Spanish DGICYT under Grant No PB93-1251, and the Programa de Cooperación con Iberoamérica.

References

- [1] Ando T, Fowler A and Stern F 1982 *Rev. Mod. Phys.* **54** 437
- [2] Sigga E D and Kwok P C 1970 *Phys. Rev. B* **32** 1024
- [3] Vinter B 1976 *Phys. Rev. B* **13** 4447
- [4] Vinter B 1977 *Phys. Rev. B* **15** 3947
- [5] Rajagopal A K 1977 *Phys. Rev. B* **15** 4264
- [6] Allen S J Jr and Tsui D C 1976 *Solid State Commun.* **20** 425
- [7] Chen W P, Chen Y J and Burstein E 1976 *Surf. Sci.* **58** 263
- [8] Tsellis A, Gonzales de la Cruz G and Quinn J J 1983 *Solid State Commun.* **46** 779
- [9] Dahl D A and Sham L J 1977 *Phys. Rev. B* **16** 651
- [10] Streight S R and Mills D L 1989 *Phys. Rev. B* **40** 10488
- [11] Wendler L and Pechstedt R 1986 *Phys. Status Solidi b* **138** 197
- [12] Wendler L and Pechstedt R 1987 *Phys. Status Solidi b* **141** 129
- [13] Wendler L, Haupt R and Grigoryan V 1988 *Phys. Status Solidi b* **149** K123
- [14] Wendler L and Grigoryan V 1989 *Solid State Commun.* **71** 527
- [15] Bloss W L 1983 *Solid State Commun.* **46** 143
- [16] Lai W Y, Kobayashi A and Das Sarma S 1986 *Phys. Rev. B* **34** 7380
- [17] Eliasson G, Hawrylak P and Quinn J J 1987 *Phys. Rev. B* **36** 7631
- [18] Nazarov V U 1994 *Phys. Rev. B* **49** 17342
- [19] Liebsh A 1987 *Phys. Rev. B* **36** 7378
- [20] Fasol G, King-Smith R D, Richards D, Ekenberg U, Mestres N and Ploog K 1989 *Phys. Rev. B* **39** 12695
- [21] Backes W H, Peters F M, Brosens F and Devreese J T 1992 *Phys. Rev. B* **45** 8437
- [22] Fernández-Velicia F J, García-Moliner F and Velasco V R 1996 *Phys. Rev. B* at press
- [23] Fernández-Velicia F J, García-Moliner F and Velasco V R 1995 *J. Phys. A: Math. Gen.* **28** 391
- [24] Ritchie R H 1957 *Phys. Rev.* **106** 874
- [25] Persson B N J 1984 *Solid State Commun.* **52** 811
- [26] Lambin P, Vigneron J P and Lucas A A 1985 *Phys. Rev. B* **32** 8203
- [27] Gumbs G and Horing N J M 1991 *Phys. Rev. B* **43** 2119
- [28] García-Moliner F and Velasco V R 1992 *Theory of Single and Multiple Interfaces* (Singapore: World Scientific)
- [29] Flores F and García-Moliner F 1979 *J. Phys. C: Solid State Phys.* **12** 907
- [30] Rocca M, Biggio F and Valbusa U 1990 *Phys. Rev. B* **42** 2835
- [31] Newns D M 1959 *Phys. Rev.* **115** 1342
- [32] Horing N J M, Kamen E and Cui H L 1985 *Phys. Rev. B* **32** 2184
- [33] Horing N J M, Fiorenza G and Cui H L 1985 *Phys. Rev. B* **31** 6349
- [34] Horing N J M and Mancini J D 1986 *Phys. Rev. B* **34** 8954
- [35] King-Smith R D and Inkson J C 1986 *Phys. Rev. B* **33** 5489